ELSEVIER

Journal of Chromatography B, 718 (1998) 15–22

JOURNAL OF CHROMATOGRAPHY B

Nonaqueous capillary electrophoresis with laser induced fluorescence detection[1]

Vicki L. Ward, Morteza G. Khaledi*

Department of Chemistry, Box 8204, North Carolina State University, Raleigh, NC 27695, USA

Received 30 November 1997; received in revised form 29 May 1998; accepted 6 July 1998

Abstract

This paper describes the use of nonaqueous capillary electrophoresis (NACE) with laser induced fluorescence (LIF) to improve detection sensitivity. The nonaqueous medium is conducive to lower detection limits due to the minimization of quenching effects. The nonaqueous solvent, *N*-methylformamide, produced the best detection limit with a 2-fold enhancement using NACE–LIF as compared to aqueous CE. *N*-methylformamide also gave the best fluorescent signal enhancement (6-fold) among the five nonaqueous solvents tested using steady-state fluorescence. The extent (or degree) of enhancement in fluorescence intensity seems to be related to the viscosity and/or polarity of the solvent.

Keywords: Nonaqueous capillary electrophoresis; *N*-Methylformamide

1. Introduction

Capillary electrophoresis (CE) is a powerful and highly efficient separation technique. Laser induced fluorescence (LIF) is a very sensitive detection method for CE that has become very applicable due to the availability of a wide variety of fluorescent tags and lasers. Detection limits for CE–LIF have been reported from attomole to zeptomole levels and as low as single molecules [1–7].

Quenching by molecular oxygen (O_2) or impurities is a problem often encountered with fluorescence detection. Two main types of quenching are dynamic and long range. Dynamic quenching occurs when an excited molecule collides with quenching species producing a nonradiative energy transfer. Dynamic quenching is diffusion controlled and is therefore dependent on the temperature and viscosity of the medium. At higher temperatures or lower viscosity, the probability of a collision occurring is amplified. Long range quenching also occurs due to a nonradiative energy transfer between molecules but without a collision. Instead, the energy transfer occurs as a result of dipole interactions between the fluorophore and quencher [8]. Overall, quenching of a sample leads to decreased signal output and results in poor detection limits. For this reason, degassing techniques such as the purge and freeze–pump–thaw methods are often incorporated into the sample preparation.

Other attempts at minimizing the quenching effect involve the use of additives in the buffer such as

*Corresponding author.

[1]Presented at the 8th Annual Frederich Conference on Capillary Electrophoresis, Frederick, MD, October, 20–22, 1997.

0378-4347/98/$19.00
PII: S0378-4347(98)00330-2

micelles and organic solvents [9–12]. Micelles have been utilized to minimize quenching via the incorporation of the fluorophore into the micelle. This shielding effect occurs as a result of the microenvironment of the micelle being more viscous compared to the aqueous bulk solution and therefore the O_2 diffusion rate is decreased and the potential of a collision is attenuated [13–15]. Additionally, increasing the micellar concentration would decrease the probability that O_2 would be present in all the micelles at the same time and thereby minimizing O_2 quenching.

Organic solvents have also been utilized to minimize quenching. The addition of organic solvents can alter the viscosity and polarity of the medium. By making the medium more viscous and less polar the dynamic and long range quenching, respectively, can be minimized. Rodríguez et al. studied the influence of organic solvents on the fluorescent signal of Se-2,3-diaminonaphthalene (Se-DAN) [12]. Their results demonstrated that as the percentage of organic solvent added to the aqueous medium was increased, a corresponding increase in fluorescent signal of the Se-DAN complex was observed. This enhancement in fluorescence was attributed to the minimization of oxygen quenching effects.

Nonaqueous capillary electrophoresis (NACE) is a relatively new area with several potential advantages that include enhanced stacking and efficiency as well as enhanced detection limits for LIF [16].

The low sample loading capacity of CE (nl volumes) can make the detection of trace amounts of sample difficult. Sample stacking is used to provide enhanced sample loading capacity that results in improved detection limits while still maintaining the resolution. NACE could be advantageous to the stacking effect due to the overall lower conductivity of many nonaqueous solvents. As a result of smaller electrical current, in nonaqueous media, separation buffers at higher ionic strengths can be utilized without the adverse effects of Joule heating.

Likewise, the lower electrical currents would allow the use of higher electric field strengths that might lead to shorter analysis times and/or better efficiencies.

The goal of this research is to demonstrate lower LIF detection limits with NACE. Lower detection limits can be achieved with a nonaqueous medium of higher viscosity and smaller polarity than with an aqueous medium.

2. Experimental

2.1. Laser fluorescence apparatus

A schematic of the fluorescence detector built in-house is shown in Fig. 1. The laser was a helium cadmium (Liconix Model 4250/10NF, Santa Clara, CA, USA) which can emit either a 7 mW 325 nm UV line or a 38 mW 442 nm blue line. The laser beam was focused by a pair of elliptical mirrors mounted on a beam steering device (Models 670RTC, 670RCB,13E20AL.2, Newport, Irvine, CA, USA) through a chopper (Model 651-1, EG&G Instruments, Trenton, NJ, USA) operated at 1000 Hz. The modulated light then enters the microscope (Model Nikon Labophot-2, Southern Micro, Atlanta, GA, USA) via an epifluorescent attachment. The chopper was used in combination with a lock-in-amplifier (Model 5105, EG&G Instruments) to filter noise from the signal. A 40× fluorite microscope objective was utilized to focus the excitation beam down onto the capillary detection window as well as to collect the resulting emission. The excitation and emission light travel through a series of filters. These filters are designed for the extraction of specific wavelengths while filtering out unwanted stray light. Once in the microscope, the excitation beam first encounters the filter cube (Model Nikon B355×, Southern Micro) that houses a 400 nm dichroic mirror and a 495 nm long-pass filter (Model Chroma

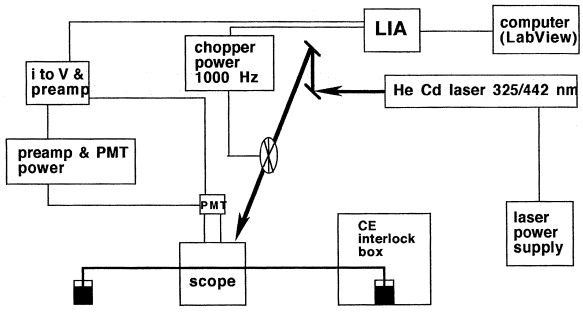

Fig. 1. Schematic of the helium cadmium laser induced fluorescence detector. PMT = photomultiplier tube; LIA = lock-in-amplifier.

400DCLP, Southern Micro). The emitted light then passes through a 515±20 nm narrow band-pass filter (Model Chroma D515/40, Southern Micro) followed by a laboratory-made 1 mm spatial filter. The filtered fluorescent light is focused onto a side on photomultiplier tube (Model R928, Hamamatsu, Bridgewater, NJ, USA) attached to the top of the microscope. The signal output from the photomultiplier passes through a current-to-voltage preamplifier (Option No. 35,PSA 01, Products For Research, Danvers, MA, USA) and enters the lock-in-amplifier. Finally, data acquisition was performed using a program written in LABVIEW (National Instruments, Austin, TX, USA).

The alignment procedure for the LIF detector was adapted from Hernandez and Escalona [17]. In order to monitor the alignment, a solution of the 8-aminonaphthalene-1,3,6-trisulfonic acid (ANTS) tag was continuously pulled through the capillary by vacuum. The microscope stage supporting the capillary detection window was translated in the *x* and *y* directions while viewing the capillary detection window through the microscope. The first step in the alignment process is to bring the capillary into focus. Then with the fluorescent tag moving through the capillary the translating and focusing is continued until a bright, fuzzy spot is observed on the capillary detection window. This intermediate portion of the alignment procedure may also require slight adjustments of the beam steering device to position the spot onto the capillary. Alignment is completed by adjusting the fine focus until the bright spot transforms into a more defined and intense diamond shape.

2.2. Steady-state fluorescence apparatus

Fluorescence spectra and intensity measurements of the fluorescent tag, ANTS, were acquired using a RF-530LPC Shimadzu spectrofluorophotometer with a xenon arc light source.

2.3. Capillary electrophoresis system

All separations were carried out on a laboratory-made CE system with LIF detection. The CE set-up consists of a 0–60 kV reversible high voltage power supply (Model SL60PN30, Spellmann, Plainview, NY, USA), a plexiglass safety interlock box to house the high voltage end of the capillary, and a LIF detector. Separations were carried out using a fused-silica capillary with a 52 μm I.D. and 365 μm O.D. (Polymicro Technologies, Tucson, AZ, USA). A −40 kV was applied to a total capillary length of 75 cm with an effective length of 47.5 cm to give a 533 V/cm electric field strength. The temperature was maintained at room temperature using a circulating oil bath (Model Lauda MA6-B, Fisher, Norcross, GA, USA). A capillary holder was also built in-house to mount the detection end of the capillary onto the microscope stage as well as to provide stability. This holder was adapted from the design given by Hernandez et al. [18]. The capillary holder is held onto the microscope stage via the stage clip and is composed of the following parts: a base plate, slider, and two smaller top plates. The capillary is placed across the base plate and secured at the ends by the two top plates using thumb tightened screws. The base plate has a hole drilled through it at the point where the capillary detection window resides. The function of the hole is to allow light through while viewing the capillary under the microscope. A slider is also located in the base plate and has a similar function to the hole. The slider can be manipulated to allow light up through the hole when viewing the capillary; however, it is kept closed during the fluorescence experiments. The base and two top plates each have a soft, black rubber lining that serves as a cushion for the capillary to prevent breakage as the top plates are screwed down onto the base plate. The holder is also painted flat black to prevent any reflective scattering of light.

2.4. Reagents and chemicals

Maltotriose and maltopentaose oligosaccharide standards were purchased from Sigma (St. Louis, MO, USA). Anhydrous citric acid, *N*-methylformamide (NMF), and formamide were purchased from Fluka (Buchs, Switzerland). The fluorescent tag ANTS was purchased from Molecular Probes (Eugene, OR, USA). Dimethylsulfoxide (DMSO), methanol, acetonitrile, glacial acetic acid, and sodium hydroxide were purchased from Fisher (Fair Lawn, NJ, USA). Sodium cyanoborohydride

($NaCNBH_3$) was purchased from Aldrich (Milwaukee, WI, USA).

2.5. Derivatization with ANTS

The ANTS derivatization procedure for the oligosaccharides was adapted from Chiesa and Horváth [19]. A 0.14 *M* ANTS solution was prepared in acetic acid–water (3:17, v/v). A 286-μl aliquot of the ANTS solution was added to an amber microcentrifuge tube already containing 100 μl of a 0.01 *M* aqueous solution of the oligosaccharide. To this mixture 200 μl of 1*M* $NaCNBH_3$ in DMSO was added. The centrifuge tube was then gently Vortex mixed and placed in a 37°C water bath for 15 h. Prior to CE analysis, the derivatized samples were filtered through 0.45 μm polypropylene filters from Scientific Resources (Eatontown, NJ, USA) and diluted to the desired concentration with 18 MΩ Milli-Q water. ANTS was an ideal tag for these experiments because its fluorescent properties, which include a maximum excitation wavelength of 353 nm and a maximum emission wavelength of 520 nm, make it ideal for the 325 nm line of the HeCd laser. Also ANTS-derivatized oligosaccharides remain charged over a broad pH range so separations can be performed under both acidic and basic conditions.

2.6. Procedure

Both aqueous and nonaqueous buffers were prepared by dissolving the appropriate amount of anhydrous citric acid to give a 100 m*M* concentration in the various solvents. The pH was adjusted to 2.5 with 1 *M* sodium hydroxide. Five 100 m*M* citric acid buffers were examined for the detection limit studies. These buffers include aqueous (prepared in water), nonaqueous (prepared in formamide and NMF), purged aqueous, and freeze–pump–thaw aqueous. During the purge degassing method, nitrogen was bubbled through the buffer aliquot for 45 min. The freeze–pump–thaw method involved first immersing the vacuum flask containing the aqueous buffer into liquid nitrogen to freeze it. A vacuum was then applied to pull off all gases above the frozen surface of the buffer. This vacuum was maintained throughout the rest of the procedure. After freezing, the buffer was allowed to thaw upon which dissolved gases rose to the surface and were extracted by the vacuum. This cycle was repeated until no more bubbles rose to the surface.

Capillary conditioning was performed at the beginning of each day by first rinsing with 1 *M* sodium hydroxide for 10 min followed by Milli-Q deionized water for 2 min and lastly with the buffer for 10 min. All samples were injected hydrodynamically for 20 s. The standards used in the calibration curves were prepared by performing a serial dilution of ANTS-derivatized maltotriose to cover a concentration range of 10^{-7} to 10^{-6} *M*. All standards were prepared in Milli-Q deionized water. Each standard was injected three times and an average was taken. A calibration curve was run for each buffer and a detection limit was calculated.

In order to enhance the precision of measurements, care was taken to minimize day-to-day changes in the fluorescent detector alignment, variation in the amount of sample injected as well as capillary overloading. Any vibrations or movement of the optical table could result in an alteration of the detector alignment which in turn would influence the fluorescence signal intensity. The potential variation in alignment was compensated for by using a control. The calibration curve for the undegassed aqueous buffer was run at the beginning of each day and used as the control for any day-to-day changes in alignment. The experiments were performed over a 4-day period after which the slopes of the control calibration curves for all 4-days were normalized with respect to the slope of day one. The normalization produced a response factor for each day representing any change in alignment. The slopes of the other calibration curves run on a particular day were then adjusted by the response factor for that day. Based on the response factors shown in Table 1 it was concluded that no significant change in alignment occurred over the 4-day period.

Table 1
Response factors for the daily alignment check

Day	Slope	Response factor
1	1.0807	1.0
2	1.0511	0.97
3	1.0530	0.97
4	1.0594	0.98

In order to compensate for variations in the injected amount of sample, an internal standard ANTS-derivatized maltopentaose, was added to all the standard solutions to a final concentration of $1.05 \cdot 10^{-6}$ *M*.

To avoid overloading the capillary, the injected plug length should not exceed 1% of the total capillary length. The plug length was calculated using Eqs. (1) and (2)

$$V_i = \frac{\Delta \rho \pi r^4 t}{8 \eta L_T} \quad (1)$$

$$\Delta p = \rho g \Delta h \quad (2)$$

where r, t, η, and L_T of Eq. (1) equal the inner radius of the capillary, injection time, viscosity, and total capillary length, respectively. In Eq. (2), ρ, g and Δh represent the sample solution density, gravitational acceleration and the height difference between the liquid levels of the sample and buffer, respectively. The volume injected for these experiments was calculated to be 2.64 nl. Once the injection volume has been determined it can be substituted into Eq. (3) to calculate the plug length (L_p) as follows:

$$L_p = \frac{V_i}{\pi r^2} \quad (3)$$

The plug length for the injections was calculated to be 0.124 cm which was 0.165% of the total column length.

Steady-state fluorescence experiments were performed by adding ANTS tag prepared in acetic acid–water (3:17, v/v) to Milli-Q deionized water and several nonaqueous solvents with and without citric acid to give a final concentration of $7.2 \cdot 10^{-5}$ *M*. The nonaqueous solvents tested were acetonitrile, methanol, DMSO, NMF and formamide. The fluorescence spectra and maximum emission intensities were measured using a spectrofluorophotometer.

3. Results and discussion

The CE–LIF calibration curves for the various conditions are compared. Slopes for the nonaqueous buffers NMF and formamide were 2-fold greater than the slope for the aqueous buffer. Degassing of the aqueous buffer using the purge and freeze–pump–thaw methods did not produce any significant change in the slope when compared to the undegassed aqueous buffer. The degassing results were first attributed to the possibility of reoxygenation of the buffer while on the CE system, since the separation buffer reservoir was open to the air at the injection end of the set-up. After further investigation using steady-state fluorescence it was revealed that the ANTS tag was potentially being quenched by the buffer itself. Although CE can be performed in pure nonaqueous solvent, it is necessary to use buffers in order to minimize band broadening effects such as electrophoretic dispersion and obtain efficient separations of ionic compounds. A 6-fold higher steady-state fluorescent signal intensity was observed for the ANTS tag in Milli-Q water over that in 100 m*M* citric acid buffer (see Table 2). Additionally, a 10-fold increase in the fluorescence signal of ANTS tag was observed for the organic solvents DMSO and methanol in the absence of

Table 2
Steady state fluorescence data for ANTS in aqueous and various nonaqueous solvents in the presence and absence of buffer

Solvent	Viscosity (mPa s) (20°C)	Polarity	Fluorescence in solvent only	Fluorescence in citrate buffer
N-Methylformamide	1.65[b]	6.0	390	246
Dimethylsulfoxide	2.20	7.2	336	27
Formamide	3.30[b]	9.6	303	230
Methanol	0.55	5.1	185	13
Acetonitrile	0.34[b]	5.8	114	[a]
Water	1.00	10.2	66	11

[a] Citrate not soluble in acetonitrile.
[b] At 25°C.
[21,22].

buffer. Given these observations, it is possible that molecular oxygen was having a negligible effect on the quenching as compared to the buffer. This would explain why the purge and freeze–pump–thaw degassing techniques used on the aqueous buffer solution with CE–LIF had no effect on the slope of the degassed calibration curves when compared to the slope of the undegassed aqueous buffer.

The slope of a calibration curve is often used as a measure of analytical sensitivity. The increase in the slope of the nonaqueous calibration curves is an indication of fluorescence enhancement. Detection limit calculations were performed using the Foley–Dorsey method given by Eqs. (4) and (5)

$$\mathrm{LOD} = \frac{3S_B}{m} \tag{4}$$

$$S_B = \frac{N_{p-p}}{5} \tag{5}$$

where m is the slope of the calibration curve and S_B represents one-fifth of the peak-to-peak noise of the baseline [20]. The detection limit results are shown in Fig. 2. The detection limit for ANTS-derivatized maltotriose was indeed reduced in the presence of the nonaqueous buffers (NMF and formamide) over that of the aqueous and degassed aqueous buffers. The enhancement in fluorescent intensity produced by the nonaqueous media is attributed to the increased viscosity and decreased polarity of both formamide and NMF compared to water. Viscosity and polarity values for the various solvents are given in Table 2. Fig. 3 supports this by showing the detection limit dependency of ANTS-derivatized maltotriose on the viscosity and polarity trends of the solvents. The detection limit decreases as the viscosity of the medium increases and as the polarity decreases. By increasing the viscosity, the mobilities of the fluorophore and the potential quenchers are decreased which in turn reduces the probability of a collision that could result in a nonradiative energy transfer. Long range quenching is also minimized due to the decrease in polarity of the nonaqueous media.

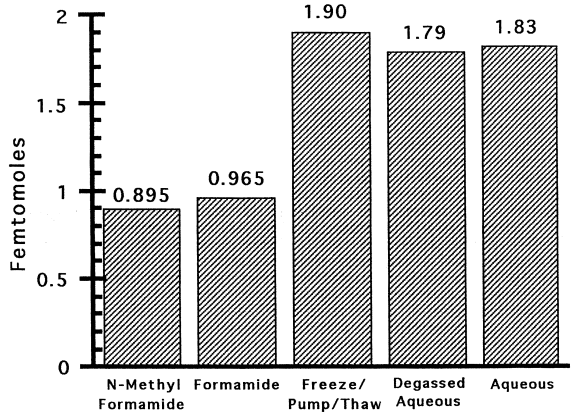

Fig. 2. CE–LIF detection limits for ANTS-derivatized maltotriose in aqueous, degassed, and nonaqueous buffers. Nonaqueous buffers produced the lowest detection limits.

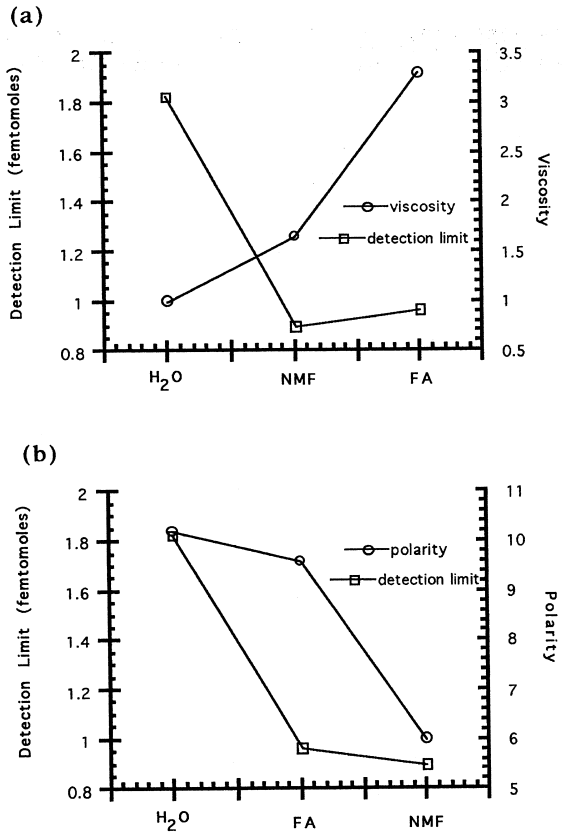

Fig. 3. Viscosity and polarity trends for the detection limit of ANTS-derivatized maltotriose. Viscosity and polarity values are shown in Table 2. The detection limit decreases with a decrease in polarity and a increase in viscosity.

Steady-state fluorescence experiments were also performed with and without citrate buffer to obtain fluorescence data for a wider range solvents (see Table 2). These results also demonstrate how the fluorescence intensity varies with the viscosity and polarity of the medium. Based on the trends shown in Table 2 with no buffer present, it is the combination of viscosity and polarity that determines the overall fluorescence intensity enhancement. Ideally, one would want high viscosity and low polarity to minimize dynamic and long range quenching. We observed that if only one condition is met then the amount of enhancement in fluorescent intensity compared to water is not as significant, with the exception of the solvent formamide. Additional evidence for the combined effects of polarity and viscosity is given by the fact that NMF, which is not the least polar or most viscous, produced the greatest enhancement. NMF produced a 6-fold increase in the steady-state fluorescent intensity of ANTS compared to water. Formamide and DMSO were ranked as second highest with a 4.5 and 5-fold enhancement respectively. It is also important to note that the steady-state fluorescence results for formamide and NMF in the absence of buffer agree with those obtained by the NACE–LIF experiments with respect to the order of the solvent enhancement; however, they differ in the degree of enhancement. A possible reason for this difference can be attributed to the quenching effects of the citrate buffer used in the CE–LIF studies. Although in these experiments it was concluded that the buffer was causing quenching, it is still a necessary component of CE separations. Therefore, in order to achieve better LOD with CE–LIF, the type and possibly concentration of buffer should be optimized to minimize quenching.

4. Conclusion

This paper demonstrated an advantage of NACE in providing lower detection limits when coupled with laser induced fluorescence. The increase in fluorescent intensity in the presence of various nonaqueous solvents is attributed to the minimization of quenching effects. The degree of fluorescent signal enhancement obtained varies from solvent to solvent and depends on the viscosity and polarity values.

Acknowledgements

We gratefully acknowledge a research grant from the National Institutes of Health (GM38738). We also thank Carsten Mundt and Paul Goode of the Electrical Engineering Department at North Carolina State University for their assistance in programming LABVIEW and Amir Malek of the Chemistry Department for assisting in the optimization of the CE–LIF system.

References

[1] Y.F. Cheng, N.J. Dovichi, Science 242 (1988) 562–563.
[2] J.Y. Zhoa, D.Y. Chen, N.J. Dovichi, J. Chromatogr. 608 (1992) 117–120.
[3] B.B. Haab, R.A. Mathies, in: E.R. Menzel, A. Katzir (Editors), Proceedings of Fluorescence Detection IV, February 1996, San Jose, CA, 1996, p. 162–169.
[4] M. Orrit, J. Bernard, R. Brown, L. Fleury, J. Wrachtrup, J. Lumin. 60 (1994) 991–996.
[5] S. Nie, D.T. Chiu, R.N. Zare, Science 266 (1994) 1018–1021.
[6] D.C. Nguyen, R.A. Keller, J.H. Jett, J.C. Martin, Anal. Chem. 59 (1987) 2158–2161.
[7] Y.H. Lee, R.G. Maus, B.W. Smith, J.D. Winefordner, Anal. Chem. 66 (1994) 4142–4149.
[8] J.D. Ingle, S.R. Crouch, in: Spectrochemical Analysis, Prentice-Hall, New Jersey, Ch. 12, 1988.
[9] H. Singh, W.L. Hinze, Anal. Lett. 15 (1982) 221–243.
[10] G.A. Davis, J. Am. Chem. Soc. 94 (1972) 5089.
[11] W.L. Hinze, Solution Chemistry of Surfactants, Plenum Press, New York, 1979, p. 104–107.
[12] E.M. Rodríguez, M.S. Alaejos, C.D. Romero, Anal. Chim. Acta 334 (1996) 161–166.
[13] G.G. Guilbault (Editor), Practical Fluorescence, Marcel Dekker, New York, 1990, p. 27–32, 158–159.
[14] M. Gratzel, J.K. Thomas, J. Am. Chem. Soc. 95 (1973) 6885.
[15] K.A. Zachariasse, N.V. Phuc, B. Kozankiewicz, J. Phys. Chem. 85 (1981) 2676.
[16] J.L. Miller, M.G. Khaledi (Editor), High-Performance Capillary Electrophoresis, Ch. 15, Chemical Analysis Series, Vol. 146, Wiley, New York, 1998.
[17] L. Hernandez, J. Escalona, J. Chromatogr. 559 (1991) 183–196.

[18] L. Hernandez, R. Marquina, J. Escalona, J. Chromatrogr. 502 (1990) 247–255.
[19] C. Chiesa, Cs. Horváth, J. Chromatogr. 645 (1993) 337–352.
[20] J.P. Foley, J.G. Dorsey, Chromatographia 18 (1934) 503–511.
[21] J.T. Przybytek (Editor), High Purity Solvent Guide, 2nd ed., Burdick & Jackson Laboratories, Michigan, 1982, p. 12, 44, 46, 74.
[22] R.S. Sahota, M.G. Khaledi, Anal. Chem. 66 (1994) 1141–1146.